Water Research 169 (2020) 115216

Contents lists available at ScienceDirect

Water Research

journal homepage: www.elsevier.com/locate/watres

An innovative multistage anaerobic hythane reactor (MAHR): Metabolic flux, thermodynamics and microbial functions

Buchun Si [a, 1], Hao Yang [a, 1], Sijie Huang [a], Jamison Watson [b], Yuanhui Zhang [a, b], Zhidan Liu [a, *]

[a] Laboratory of Environment-Enhancing Energy (E2E), Key Laboratory of Agricultural Engineering in Structure and Environment, Ministry of Agriculture, College of Water Resources and Civil Engineering, China Agricultural University, Beijing, 100083, China
[b] Department of Agricultural and Biological Engineering, University of Illinois at Urbana-Champaign, Urbana, IL, 61801, USA

ARTICLE INFO

Article history:
Received 11 April 2019
Received in revised form
21 September 2019
Accepted 18 October 2019
Available online 22 October 2019

Keywords:
Biohythane
Methane
Multistage anaerobic hythane reactor
Metabolic flux
Thermodynamics analysis
Microbial structure

ABSTRACT

Biohythane production from wastewater via anaerobic fermentation currently relies on two-stage physically separated biohydrogen and biomethane reactors, which requires closed monitoring, the implementation of a control system, and cost-intensive, complex operation. Herein, an innovative multistage anaerobic hythane reactor (MAHR) was reported via integrating two-stage fermentation into one reactor. MAHR was constructed using an internal down-flow packed bed reactor and an external up-flow sludge blanket to enhance microbial enrichment and thermodynamic feasibility of the associated bioreactions. The performance of MAHR was investigated for 160 d based on biogas production, metabolic flux and microbial structure in comparison to a typical anaerobic high-rate reactor (up-flow anaerobic sludge blanket (UASB)). A biohythane production with an optimized hydrogen volume ratio (10–20%) and a high methane content (75–80%) was achieved in the hythane zone (M_H) and methane zone (M_M) in MAHR, respectively. In addition, MAHR showed a stronger capability to accommodate a high organic loading rate (120 g COD/L/d), and it enhanced the conversion of organics leading to a methane production rate 66% higher than UASB. Thermodynamic analysis suggested that hydrogen extraction in M_H significantly decreased the hydrogen partial pressure (<0.1% vol) which favored acetogenesis in M_M. Metabolic flux and microbial function analysis further supported the superior performance of MAHR over UASB, which was primarily attributed to enhanced acetogenesis and acetoclastic methanogenesis.

1. Introduction

Hythane, which is known as hydrogen-enriched compressed natural gas, has been mandated as a forthcoming energy carrier for the internal-combustion engine. Thermal efficiency of the hythane engine has proven to be much better than compressed natural gas engines while also emitting a lower level of harmful emissions (Benemann, 1996; Mehra et al., 2017). Compared with hythane produced from fossil fuels, biohythane produced from bio-waste feedstocks via two-stage anaerobic fermentation has been proposed as a promising and sustainable alternative approach (Liu et al., 2018). Recent studies have shown that flexible and controllable biohythane production can be achieved, and the primary product can be readily utilized for direct application after the removal of carbon dioxide (Krishnan et al., 2019). Various wastewater streams have been successfully used for biohythane production, including coffee manufacturing wastewater (Jung et al., 2012), cassava wastewater (Intanoo et al., 2016), palm oil mill effluent (Seengenyoung et al., 2019) and tequila vinasses (Buitrón et al., 2014). Two-stage fermentation for biohythane production has been considered superior to traditional single-stage fermentation for biogas production not only because of its production of cleaner products, but also due to its enhanced fermentation efficiency (Chatterjee and Mazumder, 2019). Schievano et al. (2014) reported that biohythane production from biomass through two-stage fermentation resulted in a significantly higher (8%–43%) energy recovery under different conditions. We previously set up a two-stage fermentation system based on typical anaerobic high-rate reactors, which confirmed an enhanced energy recovery and

* Corresponding author.
E-mail address: zdliu@cau.edu.cn (Z. Liu).
[1] These authors contributed equally to this work.

https://doi.org/10.1016/j.watres.2019.115216
0043-1354/

organics conversion compared with single-stage fermentation (Si et al., 2016). The improvement of the two-stage fermentation system could be attributed to the enhancement and optimized control of the microbial metabolism. Fontana et al. (2018) further confirmed the superiority of two-stage in comparison to single-stage anaerobic fermentation and revealed the mechanism behind this trend based on metagenomic analysis. However, two-stage fermentation for biohythane production usually involves two physically separated reactors for biohydrogen and biomethane production. For example, previous studies have combined a continuous stirred tank reactor (CSTR) with upflow anaerobic sludge blanket (UASB) (Montiel Corona and Razo-Flores, 2018), two UASB (Intanoo et al., 2016), an anaerobic sequencing batch reactor (ASBR) with UASB (Seengenyoung et al., 2019), and two packed bed reactors (PBR) (Si et al., 2016). In addition, complicated monitoring (online pH sensing), control systems (control valves and pumps) and chemical reagents are usually required for these types of systems (Ravi et al., 2018; Seengenyoung et al., 2019). Thus, the implementation of these systems and inputs may lead to intensive operating and maintenance costs.

Integrating two-stage fermentation into a bioreactor is an attractive concept. Theoretically, the new reactor design could be based on two typical and widely used anaerobic high-rate reactors, such as the PBR (Bertin et al., 2010) and the UASB (Lettinga and Pol, 1991). However, choosing proper separation approaches for hydrogen/hythane and methane production into one system leads to design challenges for this type of reactor. The previously reported main approaches (Table A1) for fermentation separation included: (1) pretreatment of the inoculum for biohydrogen production, such as heat treatment, acid and base shock, etc., to enrich spore-forming hydrogen-producers (Wang and Yin, 2017). However, these methods could not suppress hydrogen-consuming reactions for long-term operation, especially for high-rate anaerobic reactors which had a long sludge retention time (Si et al., 2015); (2) pH control has been proven to be effective (Si et al., 2016). The optimal pH for most hydrogen bacteria ranged from 4 to 6 (Sivagurunathan et al., 2016), whereas the optimal pH value was neutral for biomethane production. However, maintaining this pH gradient would significantly increase the economic input due to the need for an online monitoring and control system. Moreover, the addition of extra chemicals for pH adjustment may lead to a digestate with a high concentration of salts which cannot be used as bio-fertilizer (Krishnan et al., 2019); (3) hydraulic retention time (HRT) control has been proposed as a possible method to separate hydrogen and methane production. The HRT for hydrogen production is much shorter than that of methane production (Table A1). In particular, the ratio of the HRT for methane production to that of hydrogen production ranged from 1 to 10. Pakarinen et al. (2011) proved that the methanogenic process can be shifted towards hydrogen production by decreasing the HRT. Si et al. (2015) investigated the effect of HRT on biohydrogen production in high-rate reactors, and the results showed that the decrease of the HRT increased the biohydrogen yield and decreased the methane production. The HRT difference during two-stage fermentation could be easily achieved via two separate reactors. However, further design changes are needed to achieve the successful implementation of an integrated bioreactor.

Considering all of this as a whole, a multistage anaerobic hythane reactor (MAHR) was proposed in this study (Fig. 1a). MAHR consisted of two zones: an inside reaction zone for biohydrogen/biohythane production (M_H) and an outside reaction zone for biomethane production (M_M). MAHR was designed based on four hypotheses/preconditions: (1) MAHR could be separated into two-reaction zones (M_H and M_M) by HRT differences. M_H could be maintained at a much lower HRT than M_M; (2) The flow pattern of the wastewater stream in the MAHR was similar to a plug flow reactor with axial dispersion, which has been considered to have hydrodynamic behaviors similar to typical high-rate anaerobic rectors (Ren et al., 2008). The wastewater flow through M_H and M_M could be conducted in sequence (red arrows) (Fig. 1a); (3) M_H could be packed with microbial carriers and it could enrich robust hydrogen producers in the form of biofilms. The packed bed biofilm reactor has been proven for continuous hydrogen production, and his type of reactor could suffer from a low HRT (reaching up to 2 h) (Si et al., 2015); (4) M_M could consisted of a granular sludge blanket, which has been verified to efficiently convert volatile fatty acids (VFAs) and alcohol generated during hydrogen production (Han et al., 2005; Si et al., 2016). As such, a novel MAHR bioreactor, which integrated two-stage fermentation into a bioreactor to continuously produce biohythane, was established based on the above hypotheses. MAHR that separated hydrogen/hythane and methane production via HRT differences reduced the economic input in comparison to conventional two-stage fermentation. In addition, an enhanced fermentation efficiency was achieved in MAHR compared with that of typical anaerobic high-rate reactors. This attributed to the advantageous ability of this reactor to include a stage-separation process. To evaluate the performance of MAHR, long-term operation (160 days) of this reactor was conducted using a UASB as the control, under identical operating conditions. This study specifically emphasized the impacts of this reactor with regard to gas production, metabolic flux, thermodynamics and microbial structure.

2. Materials and methods

2.1. Experimental setup and operation

The experiments were carried out via two laboratory scale MAHR and UASB reactors (Fig. 1). Both of the reactors were made of transparent acrylic with an effective volume of 2 L and a height-to-diameter ratio of 4:1. MAHR consisted of an inside section for hydrogen/hythane production (M_H) and an outside section for methane production (M_M). The ratio of the volumes of M_H to M_M was set at 1:3, which led to a HRT ratio of 3. This designed HRT ratio was within the range of 1–10 based on the literature (Table A1). Poly-ethylene rings were packed in M_H to serve as a microbial carrier. MAHR and UASB were maintained at mesophilic condition (37 °C) using a water jacket. Gas volumes of the two reactors were measured daily using gas meters at room temperature (25 ± 3 °C) and corrected under standard conditions (273.15 K, 101.325 kPa). The produced gas was collected in air-tight bags for composition analysis. The effluents from the reactors were first centrifuged at 4000 rpm for 10 min and then filtered using a 0.45 μm membrane filter before total organic carbon (TOC), inorganic carbon (IC) and volatile fatty acids (VFAs) analysis.

The UASB and M_M were inoculated with granular sludge obtained from a continuously operated UASB using synthetic wastewater. The same granular sludge was also used for the inoculum of the M_H zone after heat pretreatment (100 °C, 15min). The inoculum of UASB/M_M and M_H consisted of a volume inoculation ratio of 20% (v/v) and 60% (v/v), respectively. The UASB and MAHR were continuously operated using synthetic wastewater. The synthetic wastewater consisted of glucose (carbon source) and NH_4Cl (nitrogen source) with varying concentrations depending on the reactors' operational conditions. The carbon/nitrogen ratio was adjusted to 25. Nutrients were added which contained (mg/L): K_2HPO_4 250, KH_2PO_4 250, $MgCl_2$ 300, $CoCl_2$ 25, $ZnCl_2$ 11.5, $CuCl_2$ 10.5, $CaCl_2$ 25, $MnCl_2$ 15, $NiSO_4$ 16 and $FeCl_3$ 25 (Si et al., 2016). $NaHCO_3$ was added into the wastewater as a pH buffer at 1 g/g COD.

The UASB and MAHR were started up at an initial feedstock

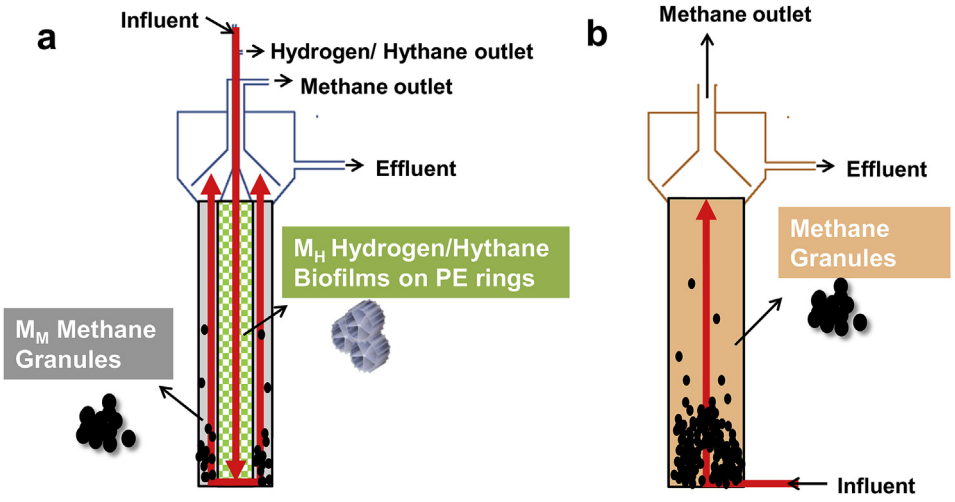

Fig. 1. Schematic description of MAHR (a) and UASB (b). The red arrows represent the directions of liquid flow, the reaction zone for hydrogen/hythane production (M_H) and the reaction zone for methane production (M_M). (For interpretation of the references to colour in this figure legend, the reader is referred to the Web version of this article.)

concentration of 2 g COD·L^{-1} and a HRT of 24 h (Fig. 2, phase 1). The feed concentration increased to 5 g COD·L^{-1} (phase 2) after the effluent's pH recovered from the initial organic shock (Fig. 2). The HRT decreased to 12 h in phase 3, and further increase of the organic loading rate (OLR) was conducted by increasing the feed concentration from 5 g COD·L^{-1} to 10 g COD·L^{-1} (phase 4). The reactors operated in phases 5–11 had an HRT of 8, 6, 4, 12, 2 and 6 h, respectively, and a fixed concentration of the feedstock (10 g COD·L^{-1}) was applied in all these phases (Fig. 2).

2.2. Analytical methods

The gas content of hydrogen, methane and carbon dioxide was determined daily via gas chromatography (SP-6890, Lunan Technologies, China). The gas chromatography system was equipped with a thermal conductivity detector and a stainless steel column packed with TDX-01. The concentration of TOC and IC was determined by a TOC analyzer (TOC-VCPN, Shimadzu, Japan). The VFAs in the effluents were analyzed by high performance liquid chromatography (Shimadzu 10A, Japan) equipped with an ultraviolet detector and a synergi 4u Hydro-RP (Phenomenex) column. Five mM H_2SO_4 was used as the mobile phase at a flow rate of 1 mL/min, and the oven temperature was set at 40 °C.

The microbial samples in UASB, M_H and M_M were collected for morphology observation and microbial diversity analysis. The microbial morphology was observed by scanning electron microscopy (SEM) (Quanta 200, FEI, USA) as previously described (Liu et al., 2012). The microbial diversity was analyzed via Illumina MiSeq sequencing. Primers 338F (5′-ACTCCTACGGGAGG CAGCAG-3′) and 806R (5′-GGACTACHVGGGTW TCTAAT-3′) for the bacteria were used. Primers Arch524F (5′-TGYCAGCCGCCGCGGTAA-3′) and Arch958R (5′-YCCGGCGTTGAVTCCAATT-3′) for the archaea were used. The PCR process was conducted as previously described (Si et al., 2015). Amplicons were extracted from 2% agarose gels and

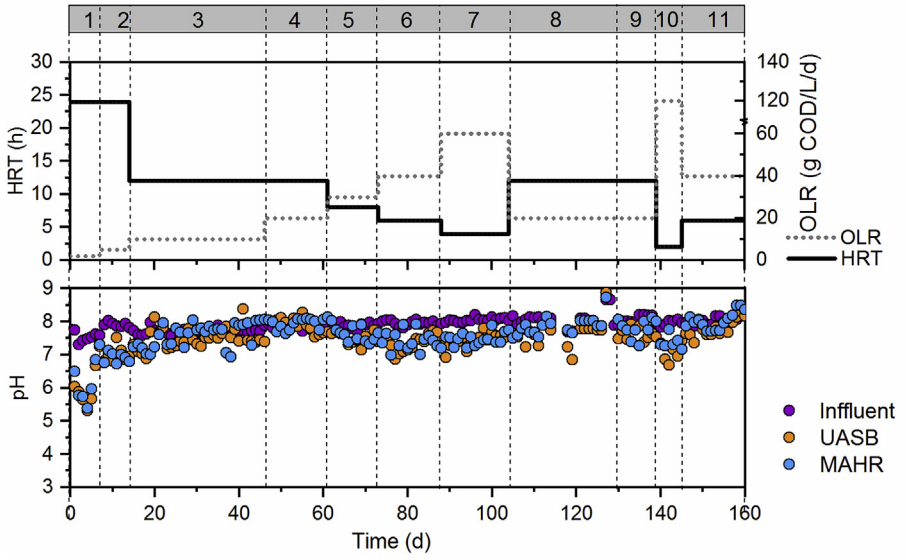

Fig. 2. Organic loading rate (OLR), hydraulic retention time (HRT) and pH value changes in MAHR and UASB during 160 days' operation. The UASB and MAHR were started up at an initial feedstock concentration of 2 g COD·L^{-1} and a HRT of 24 h (phase 1). The feed concentration increased to 5 g COD·L^{-1} (phase 2). The HRT decreased to 12 h in phase 3, and further increase of OLR was conducted by increasing the feed concentration from 5 g COD·L^{-1} to 10 g COD·L^{-1} (phase 4). The HRT (12-2 h) and OLR (20–120 g COD·$L^{-1}d^{-1}$) both varied with a fixed concentration of the feedstock (10 g COD·L^{-1}) in phase 5–11.

purified using an AxyPrep DNA gel extraction kit (Axygen Biosciences, USA) and quantified using QuantiFluor ST (Promega, USA). Purified amplicons were pooled in equimolar amounts and paired-end sequenced on an Illumina MiSeq platform. The raw reads were deposited into the National Center for Biotechnology Information (NCBI) Sequence Read Archive (SRA) database. Raw fastq files were demultiplexed and quality-filtered using Quantitative Insights into Microbial Ecology (QIIME). The phylogenetic affiliation of each 16S rRNA gene sequence was analyzed by a RDP Classifier (http://rdp.cme.msu.edu/) against the silva (SSU115) 16S rRNA database using a confidence threshold of 70%.

2.3. Calculation

The standard Gibbs free energy ($\Delta G^{0\prime}$) of bioreactions during anaerobic fermentation was collected according to the literature (Table A2). The standard conditions are 25 °C, a pressure of 1 atm, and a pH of 7. The environmental Gibbs free energy (ΔG) was calculated according to (McCarty, 1986).

$$\Delta G = \Delta G^{0\prime} + \mathrm{RT}\sum_{i=1}^{m_k} v_{ik} ln\ a_i$$

where v_{ik} is the stoichiometric coefficient for component i in reaction k with m_k components; a_i is the physiological concentrations of i; R is the universal gas constant; and T is the absolute temperature. The effect of pH was not considered for calculation of ΔG during the fermentation process because the pH of the influent and effluent was around 7 due to the addition of a pH buffer (Fig. 2).

The electron flux of MAHR and UASB was proposed based on a previous study (McCarty, 1986). Only the most significant pathway in anaerobic fermentation was proposed, though there are other pathways contributing to the production of methane. The methane production in M_H was assumed to be dominated by the hydrogenotrophic pathway, based on the results of thermodynamics analysis and microbial distribution in M_H. The distribution of the electron flux of hydrogen and methane production in M_H was calculated based on the experimental data. The calculation of the electron flux was based on the method proposed by Rittmann and McCarty (2001), and the microbial growth was not included in the analysis since the most of electron in the reaction (92%) contributed to methane.

3. Results and discussion

3.1. Operational performance of MAHR and UASB in response to different organic loads

MAHR showed separated gas production in M_H and M_M (Fig. 3a). MAHR and UASB had a similar total gas production rate from phase 1 to 5. Note that the unstable performance of MAHR at 70–130 days (phase 6–8) was mainly caused by the blockage of the gas outlet of M_H (Fig. A1), which may have occurred due to the narrow diameter and growth of the biofilms. The blockage led to the gas emission from M_H through the gas outlet of M_M (phase 6–8). This was verified by the increased hydrogen production in M_M which was amplified due to the gas produced from M_H mixing with the gas produced from M_M (Fig. 3b). In addition, the gas misdirection may have disturbed the biochemical reactions and mass transfer in M_M. Generally, MAHR had a similar or even lower gas production than UASB when M_H didn't function properly (phase 6–8). After enlarging the gas outlet of M_H (phase 9), the gas production in MAHR recovered to similar values in phase 4, which had the same HRT and OLR as phase 9. This indicated the quick recovery of MAHR from the organic loading shock (phase 5–7, 60 g $COD \cdot L^{-1}d^{-1}$). In comparison, UASB maintained a much lower gas production rate in phase 8–9 than that in phase 4 even at the same OLR. This suggested that UASB had not yet recovered from the organic loading shock. When the HRT decreased to 2 h (phase 10), a significant production of hydrogen in UASB was observed. This indicated the shift of metabolites due to the reduction of the HRT (Si et al., 2015). The methane production rate dramatically decreased due to the low HRT. The methane production rate in MAHR ($18.60 \pm 1.83\ L\,d^{-1}$) was 66% higher than that in UASB ($11.21 \pm 1.16\ L\,d^{-1}$), indicating the higher organic loading capacity of MAHR in comparison to UASB. A hydrogen production rate of $0.32 \pm 0.11\ L\,d^{-1}$ in MAHR was achieved at phase 11 (HRT 6 h). Meanwhile, a methane production rate of $24.24 \pm 2.98\ L\,d^{-1}$ was achieved in MAHR, which was 111.8% higher than that of UASB. In general, MAHR exhibited a higher organic loading capacity and more efficient system recovery from organic loading shock than UASB.

The gas content in M_H demonstrated promising biohythane production results (Fig. 3 d). A slight increase of the hydrogen content was observed in M_H as the HRT decreased. In particular, the hydrogen content in M_H increased to 18% when the HRT decreased to 6 h, but it immediately decreased to 2%. This could be attributed to the hydrogen consuming reactions, such as hydrogenotrophic methanogenesis (Table A2). Similar results were observed by the biofilm reactor for biohydrogen production, in which reducing the HRT suppressed the hydrogen-consuming reactions but could not remove these bacteria (Si et al., 2015). Although the hydrogen content was not comparable with that in a separated and pH controlled hydrogen biofilm reactor (25–40%) (Si et al., 2015), a promising amount of biohythane could be achieved in M_H. The ratio of hydrogen in hythane ranged from 0 to 89%, and the adjustment of the ratio of hydrogen in hythane was related to the methane content (ranging from 15% to 20) in M_H which decreased with the reduction of the HRT. A stable ratio of hydrogen in hythane (10–20%) was achieved in phase 11 (Fig. 3d). This hydrogen to hythane ratio was within the suggested range (Mehra et al., 2017). The produced hythane is a competitive and promising fuel for existing combustion engines, and it can be used for vehicle fuels after directly removing the carbon dioxide. The difference between the gas content in M_M and UASB further confirmed the separation of hydrogen/hythane and methane production. The gas production in M_M maintained a high methane content (Fig. 3e). In particular, the methane content in MAHR ranged from 75 to 80% at a HRT of 12 h (phase 3, 4, 9). This methane content was over 20% higher than that in UASB (around 50%). The higher methane content in second stage fermentation than single stage fermentation has also been verified in our previous study (Si et al., 2016). This could be attributed to the fact that the substrate for the second stage was mainly VFAs, which could increase the ratio of methane in the produced gas based on their stoichiometric equations (Pavlostathis, 1991). In addition, limited hydrogen production (volume content below 0.1%) was observed in M_M during the stable operation phases (phase 3, 4, 9, 10 and 11). This indicated efficient conversion of VFAs to methane by hydrogenotrophic methanogens and acetogenesis bacteria. The gas produced from M_M could be purified for the production of pure methane products and could be incorporated into a natural gas pipeline, and the purification cost would be much less than conventional single-stage fermentation due to its high content of methane.

TOC conversion and VFA changes further revealed the difference between the metabolism of organics in MAHR and UASB (Fig. 4). Both MAHR and UASB had a TOC removal close to 90% after 30 days' operation, indicating the successful startup of the reactors. The TOC removal of MAHR and UASB in phase 3 reached up to $95.3 \pm 3.1\%$

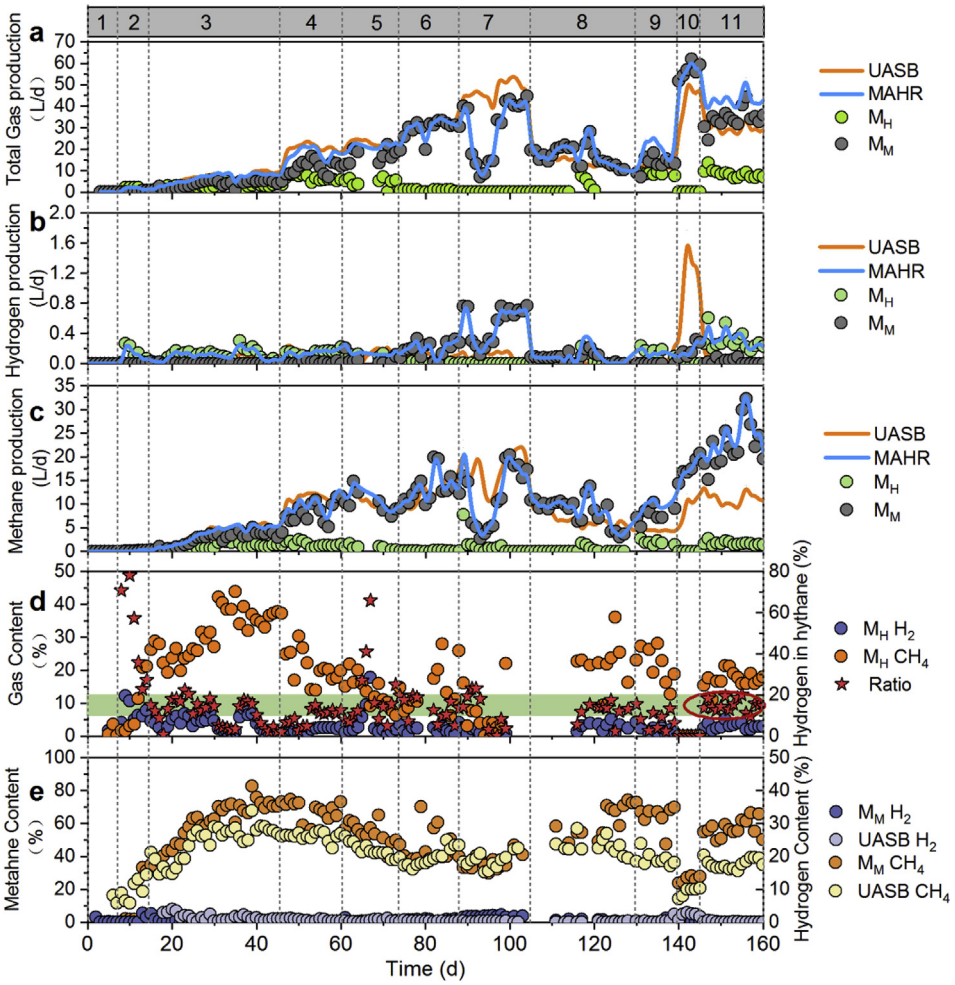

Fig. 3. Total gas production rate (a), hydrogen production rate (b), methane production rate (c) in UASB and MAHR, and the gas content in M_H (d), M_M (e) and UASB (e) during 160 days' operation. M_H is the reaction zone for hydrogen/hythane production and M_M is the reaction zone for methane production in MAHR.

and 89.7 ± 4.9%, respectively (Fig. 4a). The higher TOC removal of MAHR in comparison to UASB was also reflected by the concentration of VFAs in the effluents. A higher concentration of butyric acid was observed in UASB than MAHR (Fig. 4 b, c). This result suggested the enhanced acetogenesis in MAHR which converted butyric acid to acetic acid and hydrogen, and these products were further converted into methane. Due to the blockage of M_H (phase 6–8) as described above, the TOC removal efficiency in MAHR was similar to or even less than that of UASB, which was also confirmed by the changes in the VFAs concentration. The TOC removal in MAHR quickly recovered to 90% after the HRT returned back to 12 h (phase 9). In comparison, a TOC removal of 50% was achieved in UASB. This difference corresponded to the gas production (Fig. 3), suggesting the quicker recovery of MAHR than UASB from the organic shock. Further, the HRT decreased to 2 h (phase 10) which led to an OLR of 120 g COD·$L^{-1}d^{-1}$. A TOC removal of 38.1 ± 10.5 and 20.5 ± 6.0% was achieved in MAHR and UASB, respectively. A significant increase of VFAs was observed in MAHR and UASB. An accumulation of propionic and butyric acid was found in both MAHR and UASB. MAHR had lower concentrations of these acids than UASB, which suggested enhanced acetogenesis. In phase 11 when the HRT was changed to 6 h, a TOC removal of 75.1 ± 4.6% was achieved in MAHR, and this value was 34.7% in UASB. However, the concentration of butyric acid in MAHR dramatically decreased, whereas butyric acid in UASB remained at a similar level to that in phase 10. One interesting aspect of these results was the low concentration of acetic acid (4 ± 6 mg TOC·L^{-1}) in MAHR, whereas that in UASB reached up to 72 ± 54 mg TOC·L^{-1}. These results suggested the enhanced presence of acetogenesis and acetoclastic methanogenesis in MAHR compared with UASB. This demonstrated a promising prospective application for MAHR, since acetogenesis has been reported as one of the rate-limiting steps in anaerobic fermentation (Tommaso et al., 2015).

3.2. Thermodynamics of organics conversion in MAHR and UASB

The difference between MAHR and UASB could be further evaluated in-depth based on thermodynamics analysis. The hydrogen produced during acidogenesis was taken from the liquid phase in the form of hydrogen gas or it was further used for hydrogenotrophic methane production in M_H. The involved reactions (Table A2) had a $\Delta G^{0\prime}$ ranging from −279.4 to −164.8 kJ/mol, which indicated the thermodynamic favorability of these reactions in M_H. Note that a microenvironment may be formed in M_H among the PE rings, which may lead to insufficient mass transfer and an increased hydrogen partial pressure. In addition, unlike previous studies which maintained acidic conditions for hydrogen production (Sivagurunathan et al., 2016), MAHR was operated without pH control in this study. The added $NaHCO_3$, which acted as a pH buffer, provided a high concentration of HCO_3^- in the

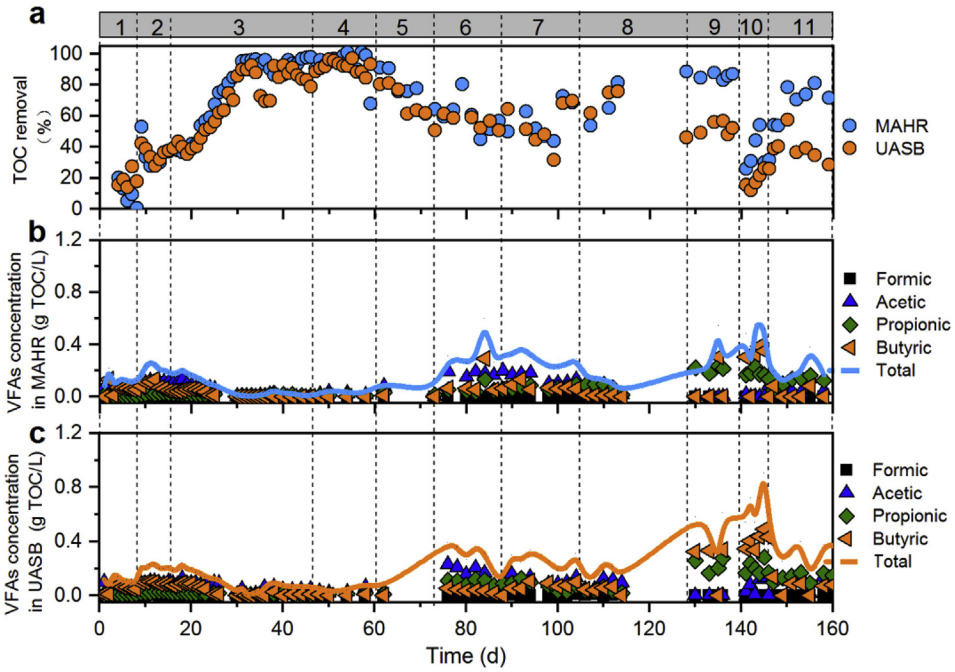

Fig. 4. TOC removal (a) and VFAs concentration (b, c) in the effluent of MAHR and UASB during 160 days' operation.

fermented liquid phase. All of the above conditions thermodynamically favored the reaction of hydrogenotrophic methanogenesis in M_H.

$$4H_2 + HCO_3^- + H^+ \rightarrow CH_4 + 3H_2O \qquad \Delta G^{0'} = -135 kJ/mol$$

Hence, it was not thermodynamically feasible to avoid methane production and produce a high content of hydrogen in M_H. However, we proved that biohythane with a proper hydrogen ratio could be achieved by reducing the HRT. The reduced HRT would improve the mass transfer in the reactor, enhance the release of hydrogen gas and further avoid conversion of produced hydrogen through methanogenesis (Si et al., 2015).

The accumulation of VFAs in M_M and UASB was found to be related to the increased hydrogen content (Fig. 5). Hydrogen partial pressure changes could significantly affect the Gibbs free energy available from the reactions during anaerobic fermentation. In particular, acetogenesis would be significantly influenced by the Gibbs free energy results (McCarty, 1986; Thauer et al., 1977). Thermodynamics quantification of acetogenesis was conducted to reveal the significant differences between the organics conversion of MAHR and UASB. After startup of UASB and MAHR from phase 1 to 5 (30 days), the ΔG of propionic acid and butyric acid acetogenesis was below zero in MAHR, suggesting well-functioning acetogenesis. This was confirmed by the organics conversion and VFAs concentration (Fig. 4). Both the ΔG of propionic acid and butyric acid acetogenesis in UASB and MAHR was above zero at phases 6–8, corresponding to the decreased TOC removal and accumulated VFAs. In particular, the ΔG of propionic acid and butyric acid acetogenesis in MAHR was higher than UASB. As discussed above, the gas outlet of M_H was blocked in phases 6–8. As a result, the produced hydrogen in M_H was rushed into M_M and increased the hydrogen partial pressure which made the process thermodynamically unfavorable for acetogenesis. In comparison, after fixing the gas outlet of M_H, the ΔG of propionic acid acetogenesis in M_M decreased to below zero in phase 9. Further decreasing the HRT to 2 h (phase 10) led to the ΔG reaching a value above zero and thereby the subsequent accumulation of propionic acid in MAHR. A similar result reported that conversion of propionic acid was kinetically difficult when a shorter HRT was adopted

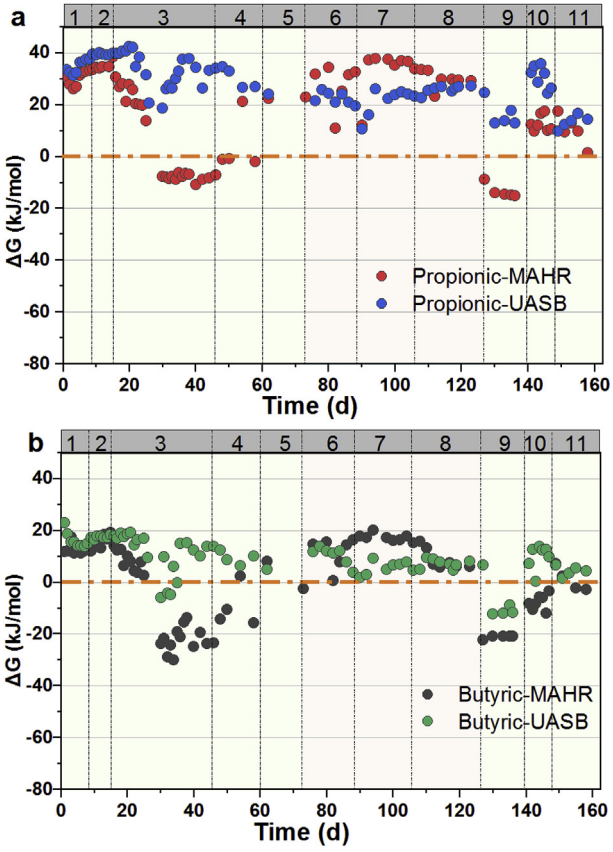

Fig. 5. Variations of environmental Gibbs free energy of acetogenesis in MAHR and UASB during 160 days' operation.

(Qiao et al., 2016). The degradation of butyric acid was more thermodynamically favored than propionic acid, which showed an environmental ΔG predominantly below zero in phases 9–11 in MAHR (Fig. 5). In general, acetogenesis in M_M was thermodynamically favorable compared with UASB, which led to a strengthened organics conversion and methane production in M_M. This was attributed to the critical role of M_H which enhanced acetogenesis in M_M via the extraction of hydrogen. Further, this also explains the reason why two-stage fermentation was more advantageous than conventional single-stage fermentation as the organic loading capacity and organic conversion increased.

3.3. Microbial community analysis

The difference between the gas production and organics conversion performance of UASB and MAHR indicated a significant difference in their microbial structure after long-term operation. SEM pictures show that the center of both granules in UASB (Fig. A2 b) and M_M (Fig. A2 f) had coccus-shaped microbes. As for the biofilm in M_H, it was dominated by rod-shaped bacteria (Fig. A2 2d). Ternary plot analysis based on Illumina Miseq sequencing further confirmed the difference between the microbial structure among M_H, M_M and UASB (Fig. 6). According to the analysis, UASB and M_H showed similar distributions of bacteria on a phylum level; both reactors contained an abundance of the enriched phylum *Firmicutes*. The phylum *Firmicutes* is usually observed in hydrogen production reactors in two-stage fermentation systems, which suggested a function of domain acidogenesis and hydrogen production (Si et al., 2016). Compared with UASB and M_H, the phylum *Proteobacteria*, *Synergistetes*, *Actinobacteria* and *Chloroflexi* were mostly associated with M_M. As for the archaea, only the phylum *Euryarchaeota* was found, and it tended to be enriched by UASB and M_M. A further comparison of the distribution of bacteria and archaea at the family level is illustrated in Fig. 7a. UASB and M_H had a much higher distribution of the family *Bacteroidaceae*, *PeH08*, *Clostridiaceae*, *Eubacteriaceae*, *Lachnospiraceae*, *Erysipelotrichaceae* and *Enterobacteriaceae* than the distribution of these families in M_M. All these bacteria were reported to be related to acidogenesis (Si et al., 2016). Some of them, such as *Clostridiaceae* and *Enterobacteriaceae,* are representative hydrogen producers (Lee et al., 2011). M_M enriched the family *Propionibacteriaceae*, *Anaerolineaceae*, *Streptococcaceae*, *Christensenellaceae*, *Syntrophomonadaceae*, *Desulfovibrionaceae*, *Syntrophobacteraceae*, and *Synergistaceae*. As for the archaea, methane producers were found in all reactor zones, which was further validated by the composition of the produced gas (Fig. 2). The family *Methanobacteriaceae* was the dominant archaea group in UASB, M_M, and M_H, and it reached its highest abundance (74.7%) in M_H. In order to further reveal the role of microbes during the metabolic pathways of organics and gas production, the relative abundance of functional bacteria and archaea was examined (Fig. 7b). Functions of dominant families were classified on the family level according to the literature (Si et al., 2016; Rosenberg et al., 2014). M_H had the highest abundance of bacteria (up to 82.94%) related to acidogenesis. In comparison, M_M had the lowest acidogenesis bacteria content. As for the acetogenesis bacteria, M_M had the highest distribution (21.69%). Acetogenesis bacteria grow in obligate syntrophy with methanogens and convert substrates that are not (or not easily) used for methane production, such as butyric and propionic acid to acetic acid and hydrogen (Stams and Plugge, 2009). These results demonstrated a dominant functional separation of acidogenesis and acetogenesis in M_H and M_M, respectively. The content of acetogenesis bacteria in MAHR was higher than that in UASB, indicating an enhanced VFAs conversion, which has been confirmed by the VFAs distribution (Fig. 4). Similar microbial distribution differences between one-stage and two-stage fermentation were also reported in a previous study when a one-stage biomethane system was shifted to a two-stage biohythane system (Si et al., 2016). The family *PeH08* in UASB reached up to 25.44%, and its function needs further investigation. For the methane producers in UASB and MAHR, the dominant archaea was related to the hydrogenotrophic methanogenesis pathway. M_H showed a high distribution of hydrogenotrophic methanogens. This corresponded to the robust methane production and low hydrogen yield in M_H (Fig. 3). In comparison, M_M contained a higher abundance of acetoclastic methanogens than M_H and UASB, which could effectively convert the acetate produced from acetogenesis. This result corresponded to the lower acetic acid concentration in the effluent of MAHR in

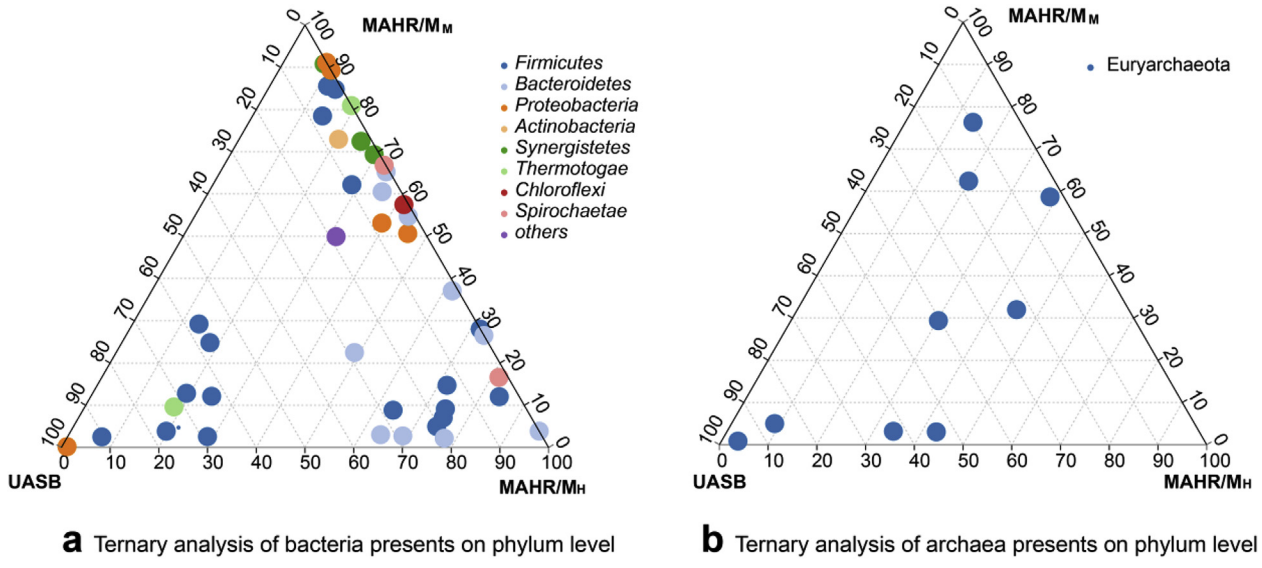

Fig. 6. Ternary plot of bacteria (a) and archaea (b) for hydrogen/hythane production (M_H), the reaction zone for methane production (M_M) and UASB. Ternary plot representing the relative occurrence of individual OTUs (circles) that are members of the phylum in M_H, M_M and UASB, respectively. The size of each circle represents its relative abundance (weighted average). The position of each circle is determined by the contribution of the indicated compartments to the total relative abundance. "Others" included phyla which were less than 0.5% of the total composition.

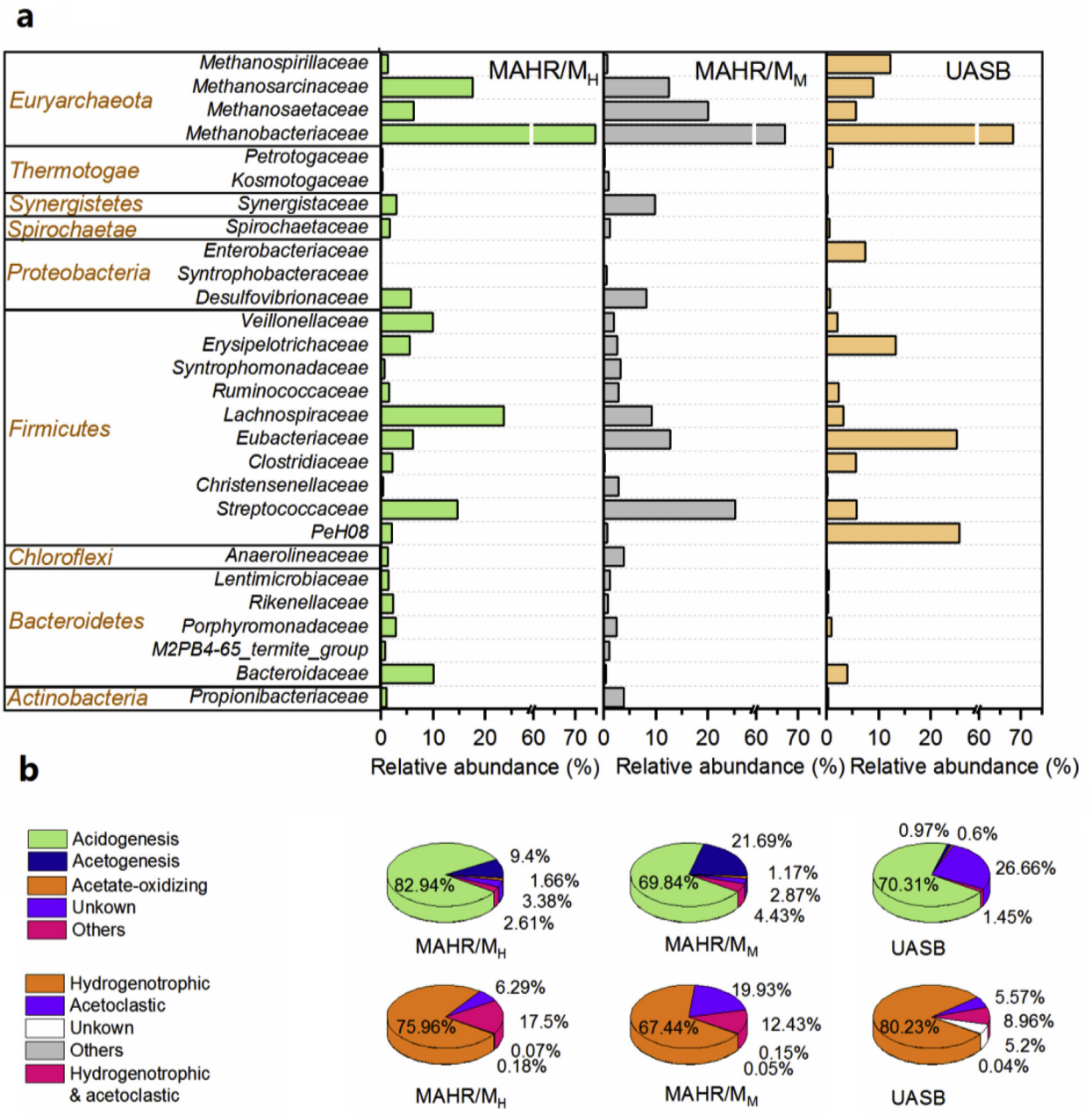

Fig. 7. Relative abundance of bacteria and archaea at the family level (a), and the relative abundance of functional microbes of bacteria and archaea (b) at the family level. "Others" included families which were less than 0.5% of the total composition. M_H is the reaction zone for hydrogen/hythane production, and M_M is the reaction zone for methane production.

comparison to UASB (Fig. 4).

Further, the microbial structure, metabolites distribution and thermodynamics were combined to reveal the biochemical pathways in UASB and MAHR (Fig. 8). Acidogenesis was the dominant biochemical reaction in M_H, which produced hydrogen and VFAs. The high content of hydrogenotrophic methanogens in M_H could be explained by its high hydrogen partial pressure, which is beneficial for hydrogenotrophic methanogenesis from a thermodynamic perspective. The low HRT in M_H tended to get rid of acetoclastic methanogens rather than hydrogenotrophic methanogens due to their much slower specific growth rate than the latter (Pavlostathis, 1991). Generally speaking, the enhanced acetogenesis and acetoclastic methanogenesis which were promoted enriching specific microbes in MAHR strengthened the organics removal and biogas production compared with UASB (Fig. 8b). This was also supported by one recent study, which found that the lower organics conversion in the single stage configuration in comparison to the two-stage fermentation was mainly correlated to the low abundance of acetogenesis bacteria and to the absence of acetoclastic methanogens (Fontana et al., 2018). In conventional UASB (Fig. 8c), the hydrogen partial pressure increases as the organic load increases. Thus, acetogenesis is easily to be inhibited from a thermodynamic perspective. Regarding MAHR, the hydrogen partial pressure remained at a low level due to the extraction of a substantial amount of hydrogen in M_H. Hence, acetogenesis was strengthened and the related microbes were enriched in M_M.

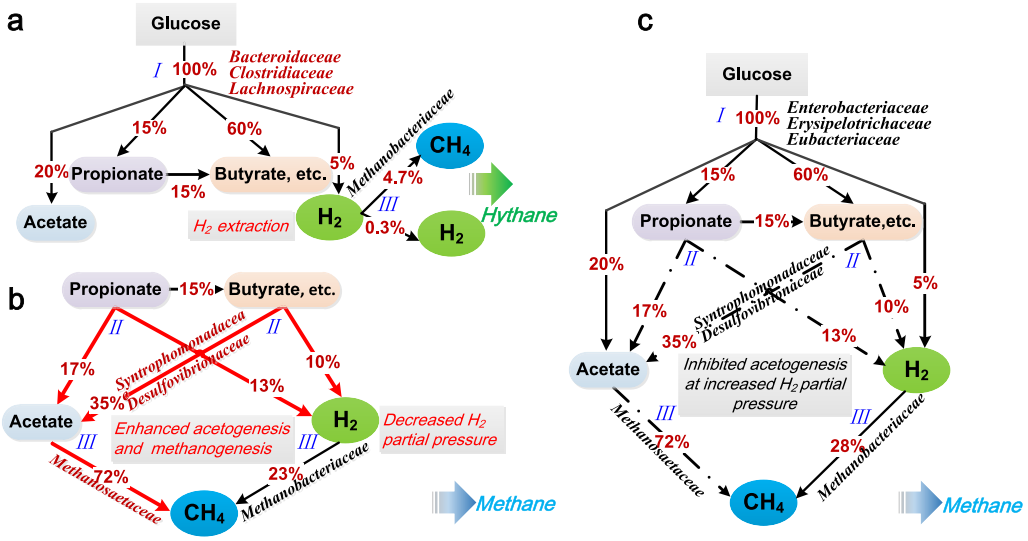

Fig. 8. Metabolic flux with functional microorganisms at (a) the reaction zone for hydrogen/hythane production (M_H), (b) the reaction zone for methane production (M_M) and UASB (c).*IIIIII* indicates acidogenesis, acetoclastic and methanogenesis, respectively. The electron flow was modified based on (McCarty, 1986).

3.4. Outlook

In this study, MAHR produced biohythane and biomethane at the same time, demonstrating advantageous aspects over traditional UASB, including a stronger tolerance to a high OLR, an enhanced organics removal, and an improved energy recovery. However, MAHR was operated with synthetic wastewater in this study, and real waste streams need to be further verified. It can be speculated that waste streams with a high content of carbohydrates would be suitable substrates for MAHR, such as palm oil mill effluent (Krishnan et al., 2017), coffee wastewater (Jung et al., 2012) and household waste (Liu et al., 2006). It's worth noting that MAHR also has potential to treat toxic wastewater, due to the fact that it demonstrated a strengthened presence of acetogenesis. The syntrophic communities consisted of acetogenesis bacteria and hydrogenotrophic methanogens known to be involved in the degradation of substrates that cannot be fermented by individual species alone (Stams and Plugge, 2009). Furthermore, these communities have also demonstrated the ability to cooperatively degrade aromatic, polyaromatic, and hydrocarbon compounds (Morris et al., 2013). Previous studies have also confirmed the active role of acetogenesis bacteria when dealing with post-hydrothermal liquefaction wastewater, which contains phenols, and N-heterocyclic compounds (Si et al., 2019). However, a waste steam containing a high concentration of metal ions, ammonia or sulfur would be a challenge for MAHR to convert. This is due to the fact that the effluent from the hydrogen/hythane production zone directly feeds into the methane production zone which would cause a shock to the sensitive methanogens. A possible manner to compensate is adjusting the methane production zone via recycling the effluent or diluting water in the section connecting the hydrogen/hythane production zones. However, these methods need further investigation. In addition, studies involving the long term (1–2 years) operation and implementation of pilot or full scale MAHR are required to ascertain if this type of reactor can be replicated in a real anaerobic fermentation system.

Another advantage is that MAHR is able of separating the hydrogen/hythane and methane production using a gradient HRT based on the reactor configuration. Hence, MAHR does not require the incorporation of an online pH detection and control system like conventional two-stage fermentation. Maintaining a pH gradient in conventional two-stage fermentation would significantly increase the economic input and is a concern for future application of the digestate. In addition, the inoculum for the startup of MAHR would be easier to implement compared to a separated two-stage high-rate reactor. There may be no requirement for heat, chemical shock or acid-base pretreatment for the inoculum of M_H to screen hydrogen production microbes, since the gradient HRT had proven could effectively separate the hydrogen/hythane and methane production and adjust the hythane production in M_H. This would avoid a significant energy and economic cost for the large scale implementation of this type of reactor (Krishnan et al., 2019). However, note that the MAHR should be designed on a case-by-case basis according to the characteristics of the feedstock. A kinetic analysis based on batch experiments is suggested before designing MAHR. In addition, the configuration for M_H and M_M should also be taken into account since the configuration would affect the sludge retention time.

The separated reaction zone in MAHR increased the complexity of the configuration compared with typical high-rate reactor. Thus, proper design of the parameters is required to avoid malfunctions. For example, the internal connection of the biohydrogen/biohythane zone and biomethane zone, which are responsible for the separated functional microbial communities (biofilms, granular sludge) and liquid products, has a complicated flow field which may lead to an unstable flow and subsequently hamper the performance of the methane production zone. In addition, the three-phase separator on top of MAHR has the potential to malfunction after long term operation (e.g. the blockage of the gas outlet of M_H in this study). Hence, the design of operational parameters based on the optimization of hydrodynamic characteristics is necessary. The optimization of hydrodynamic conditions would benefit the microbial morphology and community structure (Saur et al., 2016). For example, a higher ratio of reactor height to diameter can ensure a lon ger circular flowing trajectory, which in turn creates a more effective hydraulic attrition to microbial aggregates (Liu and Tay, 2002). In addition, the design parameters affect the mass transfer and metabolism of organics. Enhanced mass transfer can accelerate biochemical reactions by improving the contact of the microbes with the bulk solution, and it also avoids the side reactions and inhibition caused by the end products (Si et al., 2015). Another concern is that the M_H was constructed by a packed bed in this

study, which may lead to blockage after long-term operation (Speece, 1996). Hence, further improvement of the configuration of M_H is necessary.

4. Conclusion

This study demonstrated continuous biohythane production via an innovative MAHR, including two-stage fermentation in one reactor without complicated controls. MAHR could produce biohythane with a proper ratio for vehicle fuels and high content of methane at the same time. Moreover, MAHR showed a stronger capability of tolerating a high OLR and demonstrated enhanced organic conversion in comparison to conventional UASB. Metabolites flux and microbial structure analysis revealed enhanced acetogenesis and acetoclastic methanogenesis. This enhancement could be attributed to the hydrogen extraction in the hydrogen production zone which decreased the hydrogen partial pressure and thermodynamically favored acetogenesis. Further modifications of MAHR are expected and necessary in order to accommodate different feedstocks and reaction scenarios.

Declaration of competing interest

The authors declare that they have no known competing financial interests or personal relationships that could have appeared to influence the work reported in this paper.

Acknowledgements

This work was financially supported by the National Key Research and Development Program of China (2016YFD0501402), National Natural Science Foundation of China (51561145013, 51806243) and International Postdoctoral Exchange Fellowship (20170086).

Appendix A. Supplementary data

Supplementary data to this article can be found online at https://doi.org/10.1016/j.watres.2019.115216.

References

Benemann, J., 1996. Hydrogen biotechnology: progress and prospects. Nat. Biotechnol. 14, 1101–1103.
Bertin, L., Lampis, S., Todaro, D., Scoma, A., Vallini, G., Marchetti, L., Majone, M., Fava, F., 2010. Anaerobic acidogenic digestion of olive mill wastewaters in biofilm reactors packed with ceramic filters or granular activated carbon. Water Res. 44, 4537–4549.
Buitrón, G., Kumar, G., Martinez-Arce, A., Moreno, G., 2014. Hydrogen and methane production via a two-stage processes (H_2-SBR + CH_4-UASB) using tequila vinasses. Int. J. Hydrogen Energy 39, 19249–19255.
Chatterjee, B., Mazumder, D., 2019. Role of stage-separation in the ubiquitous development of anaerobic digestion of organic fraction of municipal solid waste: a critical review. Renew. Sustain. Energy Rev. 104, 439–469.
Fontana, A., Campanaro, S., Treu, L., Kougias, P.G., Cappa, F., Morelli, L., Angelidaki, I., 2018. Performance and genome-centric metagenomics of thermophilic single and two-stage anaerobic digesters treating cheese wastes. Water Res. 134, 181–191.
Han, S., Kim, S., Shin, H., 2005. UASB treatment of wastewater with VFA and alcohol generated during hydrogen fermentation of food waste. Process Biochem. 40, 2897–2905.
Intanoo, P., Chaimongkol, P., Chavadej, S., 2016. Hydrogen and methane production from cassava wastewater using two-stage upflow anaerobic sludge blanket reactors (UASB) with an emphasis on maximum hydrogen production. Int. J. Hydrogen Energy 41, 6107–6114.
Jung, K., Kim, D., Lee, M., Shin, H., 2012. Two-stage UASB reactor converting coffee drink manufacturing wastewater to hydrogen and methane. Int. J. Hydrogen Energy 37, 7473–7481.
Krishnan, S., Din, M.F.M., Taib, S.M., Ling, Y.E., Puteh, H., Mishra, P., Nasrullah, M., Sakinah, M., Wahid, Z.A., Rana, S., Singh, L., 2019. Process constraints in sustainable bio-hythane production from wastewater: technical note. Bioresour. Technol. Rep. 5, 359–363.
Krishnan, S., Singh, L., Sakinah, M., Thakur, S., Wahid, Z.A., Ghrayeb, O.A., 2017. Role of organic loading rate in bioenergy generation from palm oil mill effluent in a two-stage up-flow anaerobic sludge blanket continuous-stirred tank reactor. J. Clean. Prod. 142, 3044–3049.
Lee, D., Show, K., Su, A., 2011. Dark fermentation on biohydrogen production: pure culture. Bioresour. Technol. 102, 8393–8402.
Lettinga, G., Pol, L.H., 1991. UASB process design for various types of wastewaters. Water Sci. Technol. 24, 87–107.
Liu, D., Liu, D., Zeng, R.J., Angelidaki, I., 2006. Hydrogen and methane production from household solid waste in the two-stage fermentation process. Water Res. 40, 2230–2236.
Liu, Y., Tay, J., 2002. The essential role of hydrodynamic shear force in the formation of biofilm and granular sludge. Water Res. 36, 1653–1665.
Liu, Z., Lv, F., Zheng, H., Zhang, C., Wei, F., Xing, X., 2012. Enhanced hydrogen production in a UASB reactor by retaining microbial consortium onto carbon nanotubes (CNTs). Int. J. Hydrogen Energy 37, 10619–10626.
Liu, Z., Si, B., Li, J., He, J., Zhang, C., Lu, Y., Zhang, Y., Xing, X., 2018. Bioprocess engineering for biohythane production from low-grade waste biomass: technical challenges towards scale up. Curr. Opin. Biotechnol. 50, 25–31.
McCarty, P.L., 1986. Anaerobic wastewater treatment. Envimn. Sci. Technol. 20, 1200–1206.
Mehra, R.K., Duan, H., Juknelevičius, R., Ma, F., Li, J., 2017. Progress in hydrogen enriched compressed natural gas (HCNG) internal combustion engines - a comprehensive review. Renew. Sustain. Energy Rev. 80, 1458–1498.
Montiel Corona, V., Razo-Flores, E., 2018. Continuous hydrogen and methane production from Agave tequilana bagasse hydrolysate by sequential process to maximize energy recovery efficiency. Bioresour. Technol. 249, 334–341.
Morris, B.E.L., Henneberger, R., Huber, H., Moissl-Eichinger, C., 2013. Microbial syntrophy: interaction for the common good. FEMS Microbiol. Rev. 37, 384–406.
Pakarinen, O., Kaparaju, P., Rintala, J., 2011. The effect of organic loading rate and retention time on hydrogen production from a methanogenic CSTR. Bioresour. Technol. 102, 8952–8957.
Pavlostathis, S.G., 1991. Kinetics of anaerobic treatment: a critical review. Crit. Rev. Environ. Contr. 21, 411–490.
Qiao, W., Takayanagi, K., Li, Q., Shofie, M., Gao, F., Dong, R., Li, Y., 2016. Thermodynamically enhancing propionic acid degradation by using sulfate as an external electron acceptor in a thermophilic anaerobic membrane reactor. Water Res. 106, 320–329.
Ravi, P.P., Lindner, J., Oechsner, H., Lemmer, A., 2018. Effects of target pH-value on organic acids and methane production in two-stage anaerobic digestion of vegetable waste. Bioresour. Technol. 247, 96–102.
Ren, T., Mu, Y., Yu, H., Harada, H., Li, Y., 2008. Dispersion analysis of an acidogenic UASB reactor. Chem. Eng. J. 142, 182–189.
Rittmann, B.E., McCarty, P.L., 2001. Environmental Biotechnology: Principles and Application. McGraw-Hill.
Rosenberg, E., DeLong, E.F., Lory, S., Stackebrandt, E., Thompson, F., 2014. *Firmicutes* and *Tenericutes* the Prokaryotes. Springer.
Saur, T., Escudié, R., Santa-Catalina, G., Bernet, N., Milferstedt, K., 2016. Conservation of acquired morphology and community structure in aged biofilms after facing environmental stress. Water Res. 88, 164–172.
Schievano, A., Tenca, A., Lonati, S., Manzini, E., Adani, F., 2014. Can two-stage instead of one-stage anaerobic digestion really increase energy recovery from biomass? Appl. Energy 124, 335–342.
Seengenyoung, J., Mamimin, C., Prasertsan, P., O-Thong, S., 2019. Pilot-scale of biohythane production from palm oil mill effluent by two-stage thermophilic anaerobic fermentation. Int. J. Hydrogen Energy 44, 3347–3355.
Si, B., Li, J., Li, B., Zhu, Z., Shen, R., Zhang, Y., Liu, Z., 2015. The role of hydraulic retention time on controlling methanogenesis and homoacetogenesis in biohydrogen production using upflow anaerobic sludge blanket (UASB) reactor and packed bed reactor (PBR). Int. J. Hydrogen Energy 40, 11414–11421.
Si, B., Liu, Z., Zhang, Y., Li, J., Shen, R., Zhu, Z., Xing, X., 2016. Towards biohythane production from biomass: influence of operational stage on anaerobic fermentation and microbial community. Int. J. Hydrogen Energy 41, 4429–4438.
Si, B., Yang, L., Zhou, X., Watson, J., Tommaso, G., Chen, W., Liao, Q., Duan, N., Liu, Z., Zhang, Y., 2019. Anaerobic conversion of the hydrothermal liquefaction aqueous phase: fate of organics and intensification with granule activated carbon/ozone pretreatment. Green Chem. 21, 1305–1318.
Sivagurunathan, P., Kumar, G., Bakonyi, P., Kim, S., Kobayashi, T., Xu, K.Q., Lakner, G., Tóth, G., Nemestóthy, N., Bélafi-Bakó, K., 2016. A critical review on issues and overcoming strategies for the enhancement of dark fermentative hydrogen production in continuous systems. Int. J. Hydrogen Energy 41, 3820–3836.
Speece, R.E., 1996. Anaerobic Biotechnology for Industrial Wastewaters. Archae Press.
Stams, A.J.M., Plugge, C.M., 2009. Electron transfer in syntrophic communities of anaerobic bacteria and archaea. Nat. Rev. Microbiol. 7, 568–577.
Thauer, R.K., Jungermann, K.A., Decker, K., 1977. Energy conservation in chemotrophic anaerobic bacteria. Bacteriol. Rev. 41, 100–180.
Tommaso, G., Chen, W., Li, P., Schideman, L., Zhang, Y., 2015. Chemical characterization and anaerobic biodegradability of hydrothermal liquefaction aqueous products from mixed-culture wastewater algae. Bioresour. Technol. 178, 139–146.
Wang, J., Yin, Y., 2017. Principle and application of different pretreatment methods for enriching hydrogen-producing bacteria from mixed cultures. Int. J. Hydrogen Energy 42, 4804–4823.